九州大学学術情報リポジトリ
Kyushu University Institutional Repository

Effect of Calcination Temperature on The Properties of Eggshell Waste (EW) Powder for Biomedical Application

Razak, Aisyah
Faculty of Mechanical & Manufacturing, Universiti Tun Hussein Onn Malaysia (UTHM)

Najah Mat Isa
Faculty of Mechanical & Manufacturing, Universiti Tun Hussein Onn Malaysia (UTHM)

Kinit, Sebastian
Faculty of Mechanical & Manufacturing, Universiti Tun Hussein Onn Malaysia (UTHM)

Adzila, Sharifah
Faculty of Mechanical & Manufacturing, Universiti Tun Hussein Onn Malaysia (UTHM)

https://doi.org/10.5109/6792828

出版情報：Evergreen. 10 (2), pp.782-791, 2023-06. 九州大学グリーンテクノロジー研究教育センター
バージョン：
権利関係：Creative Commons Attribution-NonCommercial 4.0 International

KYUSHU UNIVERSITY

Effect of Calcination Temperature on The Properties of Eggshell Waste (EW) Powder for Biomedical Application

Aisyah Razak[1], Najah Mat Isa[1], Sebastian Kinit[1], Sharifah Adzila[1,*]
[1]Faculty of Mechanical & Manufacturing, Universiti Tun Hussein Onn Malaysia (UTHM), Parit Raja, 86400, Malaysia

*Author to whom correspondence should be addressed:
E-mail: adzila@uthm.edu.my

(Received November 11, 2022; Revised May 16, 2023; accepted May 22, 2023).

Abstract: Eggshell waste has been developed as a viable choice for biomaterials in bone regeneration. In this study, eggshell waste was subjected to calcination at 600°C, 700°C, 800°C and 900°C for 4 hours, resulting in the complete conversion of calcium carbonate ($CaCO_3$) into calcium oxide (CaO) powder. Using Scanning Electron Microscopy (SEM) and Image J software, mean particle size powders and hardness values via Vickers-microhardness were investigated. Notably, powder calcined at 900°C has the highest mean hardness value due to powder densifications with narrow pore size. Therefore, CaO as a source of calcium ions indicates its potential use in biomedical applications.

Keywords: Eggshell waste, biomaterial, density, hardness, biomedical application.

1. Introduction

The core foundation of researchers and scholars in this millennium is to develop efficient ecosystems and sustainable environments that are safe for humans and other living things on Earth. Making something useful out of waste, particularly from daily life and the food industry, seems impossible and of little value[1),2),3)]. Wastes should be recycled, repurposed, and used to create added-value products when considering sustainable development. Thus, exploration through research in materials science, especially in the field of waste material, has become a serious issue and has led the researcher to the point that waste from daily domestic use and the food processing industry can be transformed and converted into some helpful product and yet seems to be achievable[4)]. In the same context, eggshells are generally known as one of the most significant contributors to agricultural waste, capable of constituting environmental problems and pollution as it contributes to 250,000 tons annually worldwide in dumping areas[5),6),7)]. The efficacy of converting eggshells to productive use becomes worth adopting in the ever-increasing initiatives to convert waste into a high-value product.

Eggs are typical in many items, including desserts, fast food, and regular meals. The production of eggshells, regarded as waste in the industry, occurs during the production of chicken eggs[8),9)]. In addition, eggshell waste must be disposed of in landfills without being processed because it has no commercial value. As a result, public health and environmental contamination are hazardous. Because eggshells are part of solid waste, a high output of eggshell trash may increase solid waste production in landfills[1,10)]. In the year 2012, Malaysia produced around 642 600 tonnes of eggs. The shell accounts for about 11% of the overall weight. The shell represents 11% of the entire weight, equating to 70,686 tonnes of garbage created annually[11),12),13)]. It is anticipated that more eggshell trash will be produced each year, endangering the environment.

Eggshells primarily consist of calcium carbonate ($CaCO_3$), present in its elemental composition. An eggshell is made up of 94% $CaCO_3$ or also known as calcite form, 1% magnesium carbonate ($MgCO_3$), 1% calcium phosphate ($Ca_3(PO_4)_2$), and 4% organic material[14),15),16)]. After some research, eggshells are helpful for many applications such as biodiesel catalyst[17)], adsorbent to remove chromium[18)], reinforcement in fabricating the aluminium-based composite material[19)], and calcium precursor in calcium phosphate (CaP) production[20)].

Through the calcination process, $CaCO_3$ from eggshells can be changed into calcium oxide (CaO). Eggshells CaO is the active phase, and temperatures above 800°C are required for proper calcination[21)]. Obtaining CaO is crucial because it serves as a raw material for producing CaP or hydroxyapatite, which will then be synthesised using various synthesis techniques to manufacture scaffolds or satisfy any other biomedical requirement[20),22),23),24)].

The problem of the high volume of eggshell waste at dumping areas has led this research to convert eggshell waste to valuable material. Rather than buying CaO from the market, it is cheaper and can help to reduce the volume of eggshell waste in the dumping areas. Besides, soil and air pollution can be reduced due to the high volume of trash being dumped. This research focused on calcifying chicken eggshells at different temperatures as the primary source of $CaCO_3$ to become CaO. The relationship between calcination temperature and the materials' physical, mechanical and morphological properties was studied to find the most suitable temperature to produce CaO powder for application in CaP production.

2. Methods

2.1 Sample preparation

The eggshell waste (EW) was obtained from the Chilli Cafe at Kolej Kediaman Tun Dr Ismail (KKTDI) UTHM. After collecting the material, the eggshell was washed thoroughly using tap water. The eggshell was then boiled for 30 minutes in deionized water. It is then crushed into tiny flakes and dried for four hours at 100°C in the oven, as shown in Fig. 1.

Fig. 1: Crushed EW.

Each of the samples weighed approximately 30 g respectively before calcined. The dry EW was subjected to a 4 hours calcination process at four different temperatures (600°C, 700°C, 800°C, and 900°C), with the standard temperature increment and decrement profile. Next, the uncalcined and all calcined samples were crushed into small flakes using an electric grinder. The sample was sieved in size of < 40µm as shown in Fig. 2. To prevent a reaction from carbon dioxide (CO_2) and humidity in the air, and all samples were kept in drying boxes.

Fig. 2: EW after calcination and sieving process.

For sample preparation, 2 g of each powdered sample (uncalcined EW, 600°C, 700°C, 800°C, and 900°C) were weighed and mixed with 6 drops of Polyethylene Glycol (PEG). This mixing process continued until all the binding solutions had been incorporated. The mixed powder was poured into 13 mm diameter of molds. Then, the powder was compressed at 5 tons for 1 min. The process was repeated 5 times for 5 samples. The sample after compaction is shown in Fig. 3.

Fig. 3: Sample after compaction.

Summary of sample preparation is shown in Fig 4.

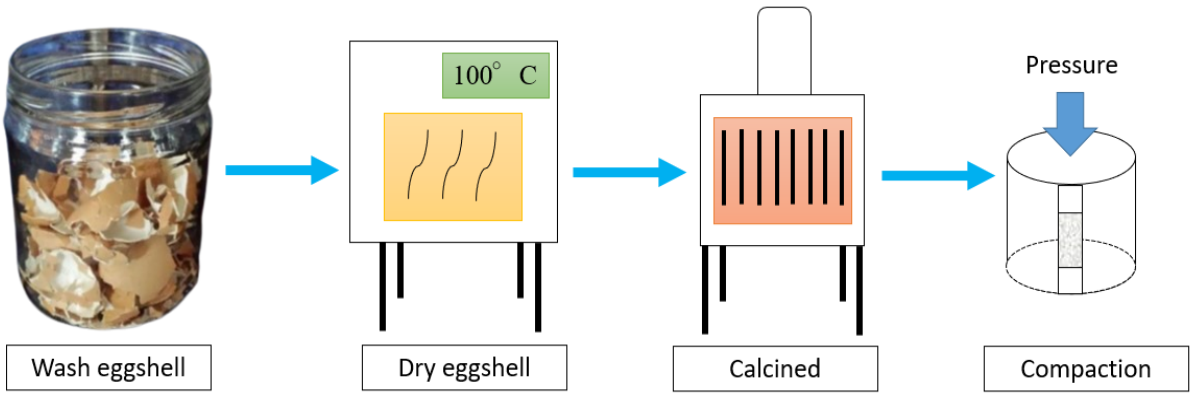

Fig. 4: Illustration of sample preparation

2.2 Porosity and density test

Pellets for all samples were weighed to record their dry weight. After that, all pellets were soaked in boiling water. Approximately 1000 ml of distilled water was filled into a 1000 ml beaker and placed under the heater (HP-16055). The distilled water was boiled until reaching a bubbling state, and the samples were ready to boil into the beaker, as shown in Fig. 5. The boiling process took 2 hours before the soaking process for 14 hours.

Fig. 5: Boiling process.

After 12 hours of soaking, the pellets were weighed. The first weighting stage was measuring the pellet's suspended mass immersed in the water. The data was collected for suspended mass. The pellet was taken out from the water and dried using filter paper. Then, the pellet was weighed again to measure the wet mass.

A water immersion method based on Archimedes' principle was used to calculate the overall porosity, density, and open porosity of the calcined samples using the following equation where P_{open} is the sample's volume fraction of open porosity, M_{wet} is the sample's mass after soaking in water, M_{dry} is the sample dry mass, $M_{suspended}$ is the sample's mass after soaking in water, $P_{overall}$ is the sample's volume fraction of overall porosity (vol. percent), and ρ is density. The analytical balance (*XS64 Mettler Toledo*) was used to make this measurement.

$$P_{open} = \frac{M_{wet} - M_{dry}}{M_{wet} - M_{suspended}} \quad (1)$$

$$P_{overall} = \left(1 - \frac{\rho}{\rho_{theoretical}}\right) \times 100\% \quad (2)$$

$$\rho = \frac{M_{dry} \times \rho_{water}}{M_{wet} - M_{suspended}} \quad (3)$$

2.3 Particle size analysis

The apparent size and morphologies of the powder samples were examined under Scanning Electron Microscopy (SEM) (*SEM-Hitachi U151O*) with 3000 X magnification by utilising a scale of 10 µm and an accelerating voltage of 15 kV. To make a conductive layer and decrease the sample's charging, all samples were double-coated with gold using a sputter coater.

For particle size distribution analysis, ImageJ software, a freeware Java-based Image Processing software, was utilized in this study. It is faster and more precise, and the image quality of the processing is good. Image Processing via image SEM may measure various size and form metrics, such as size distribution, perimeter, ferret diameter, and circularity.

2.4 Hardness test

Vickers hardness (HV) testing used the (INNOVATEST Falcon 500) microhardness tester. The indentation was observed under 40 X magnifications. HV was measured to investigate the effects of indentation load and time on the hardness values. With an indentation load of 245.2 mN and a range of indentation times from 1 to 10 s, the indentation was performed. For improved repeatability, each test indentation was repeated five times. SEM image with a scale of 10 µm was used to analyze the size of the diamond shape after the indentation process.

3. Results and Discussion

3.1 Porosity and density analysis

In porous materials, the shape of the pores is influenced by the original shape of the powder particle. The powder's particle size and shape influence the green density and

pore size distribution. The term "green density" refers to the volume of solid material divided by the total volume of the powder compact before sintering or after calcination[25]. Green bodies of fine particles typically have pore structures with pore diameters that match the calcination temperature and the size of the agglomerated particles. After calcination, the pores between primary particles may close up during the compaction process, while the pores between agglomerates continue to exist. It was found that it is possible to calculate the relative density of the porous eggshell ceramic samples. Table 1 displays the precise open pore volume and total pore volume of the reference sample of EW and all the calcined samples. It was observable that uncalcined EW had a specific pore volume for open porosity that was much higher (0.27 vol%) than that of calcined EW due to the larger pore diameter of EW; thus, it has a higher specific pore volume. However, the specific pore volume of calcined EW decreased at 600°C, 700°C, 800°C, and 900°C.

Table 1. Open and total pore volume and green density of EW samples.

Temperature (°C)	**Poverall (vol%)**	**Popen (vol%)**	**Green density, ρ_G (g/cm^3)**
Uncalcined	29.6420	0.2688	±2.5113
600	2.5643	0.1726	±2.1526
700	4.6037	0.1371	±2.1526
800	13.3931	0.1336	±2.1526
900	14.0342	0.0972	±2.1526

Based on Fig. 6, the graph's trend indicates that the porosity line drastically drops from 600°C to 700°C and then gradually drops to 800°C. Then, from 800°C to 900°C, the line sharply dropped. These lines trend was anticipated because; using PEG as a binder would unfavorably intact the particle to give a minuscule size of pore area of the sample, and the homogeneous size of particle that existed less than 10 µm influences the particle composition to become more rigid and reduces the open gap between particles due to thermal decomposition upon higher temperature. The specific surface area and pore volume shrank as the calcination temperature rose[26,27,28]. The most significant specific open pore volume of EW produced at 600°C (0.17 vol%) was around two times lower than that of uncalcined EW (0.26 vol%). The bigger $CaCO_3$ pore sizes were used to accommodate the size of the eggshell's natural pores and, more critically, the spaces between the calcined EW matrices.

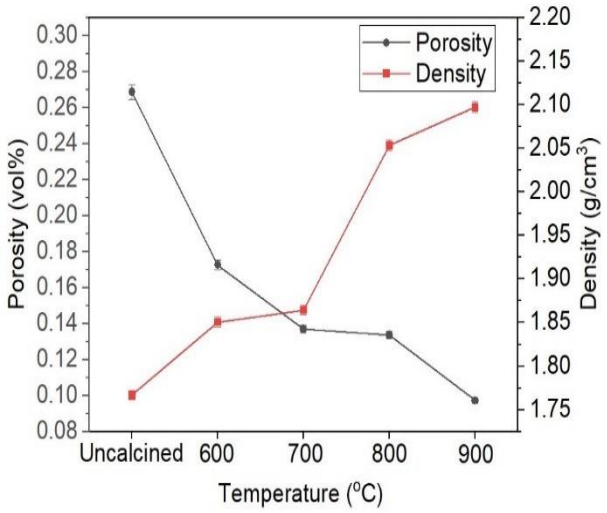

Fig. 6: Porosity density vs calcination temperature graph.

Next, the density value of both samples revealed that uncalcined EW has a lower density than calcined. EW samples. It is caused by the uniform size and shape of the particles and compositional arrangement. More pores are often produced when a particle has a higher specific surface area. It demonstrates that for calcined EW, the density increased from 600°C to 900°C, as seen by the density trend line in Fig. 6. According to the graph, the line rose steadily starting at 600°C and then abruptly peaked at 800°C before gradually raised as it approaches 900°C. Besides, EW did not wholly decompose to CaO after calcination at 600°C, instead producing a mixed catalyst with $CaCO_3$ as the peak existence of XRD revealed in the previous study[1]. Small CaO and larger $CaCO_3$ particles combine to form a finer composition that can close small gaps and create pores that are fewer than 50 nm in size. However, 900°C homogenous size particles are around 10 µm less dense than 600°C-sized particles. When comparing samples' relative density (RD), all calcined pellet shows significantly higher RD value contrary to uncalcined EW pellet. The highest RD value was 97.4357% at 900°C calcination temperature, while the lowest RD value recorded at uncalcined EW pellet was 70.3580%. It suggests that a more significant temperature causes a higher RD value. Thus, pellets that undergo calcination tend to get denser.

3.2 Particle size analysis

The apparent size and morphologies of both uncalcined and calcined EW before compaction (BC) and after compaction (AC) samples were analyzed. Fig. 7 (a) to (e) shows all samples before compaction that are in powder form and have a surface with unevenly shaped rock-like particles, which is similarly related to our earlier work[1]. The uncalcined EW (Fig. 7 a), composed of microscopic particles of $CaCO_3$, was found surrounding rock-shaped particles with flat and asymmetrical surfaces, showing that the size of the uncalcined sample was not uniform. This concrete stone-like shape was observed as

calcination temperature increased up to 700°C, where the physical surface of the structural composition was uneven and appeared to have wholly degenerated into disorder. The shape of the powder gradually changes as the edges become more rounded, starting at a calcination temperature of 800°C and the highest calcination temperature of 900°C; the shape of the powder changed due to heat treatment to an interconnected skeleton shape from irregular flakes. According to the surface morphology of the sample after compaction, the disappearance of the grain boundary in Fig. 7 (a') to (e') starting from the uncalcined EW is primarily due to the powder's mean size decreasing with the calcination temperature and the aid of the PEG binder used during the compaction process.

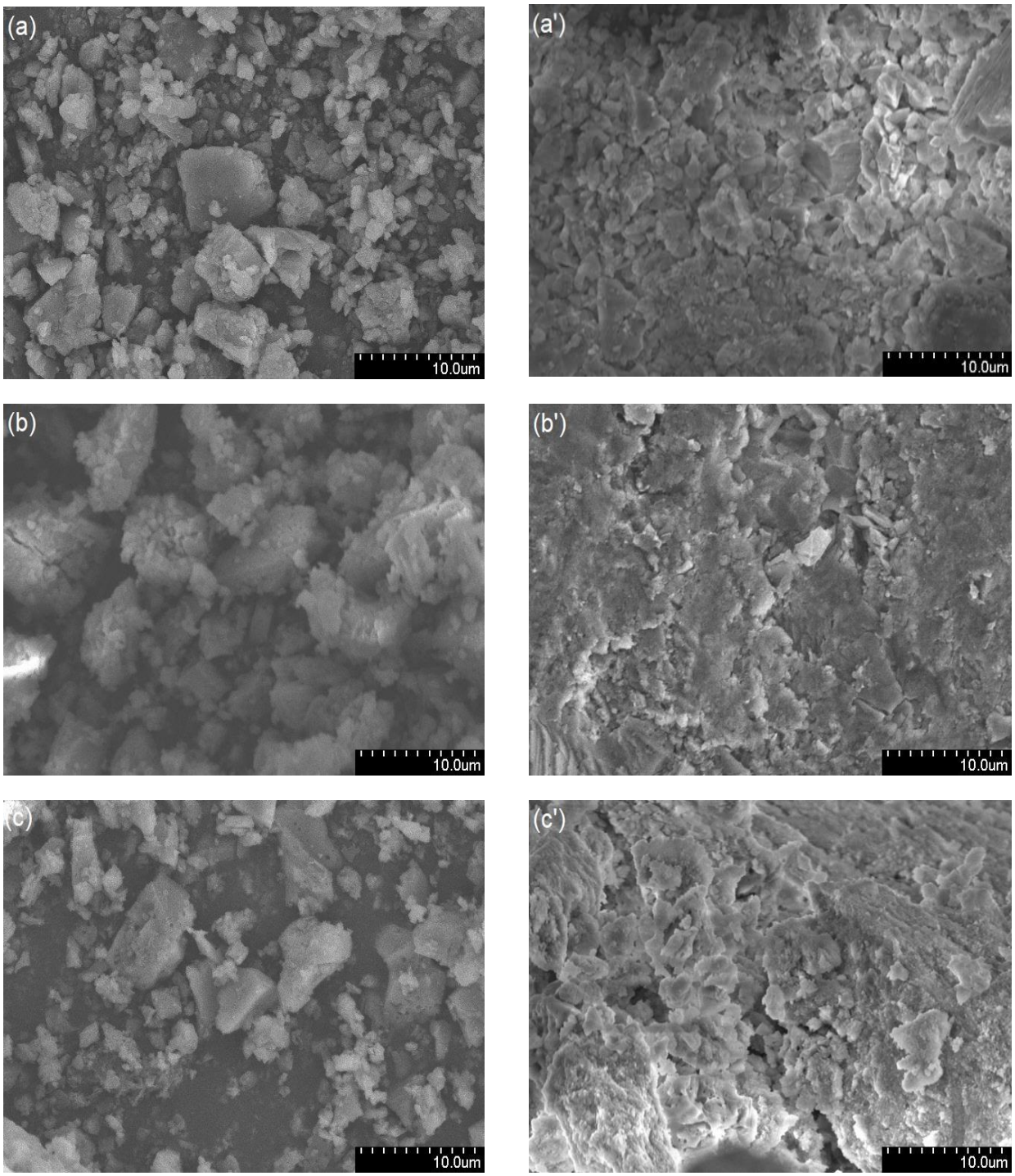

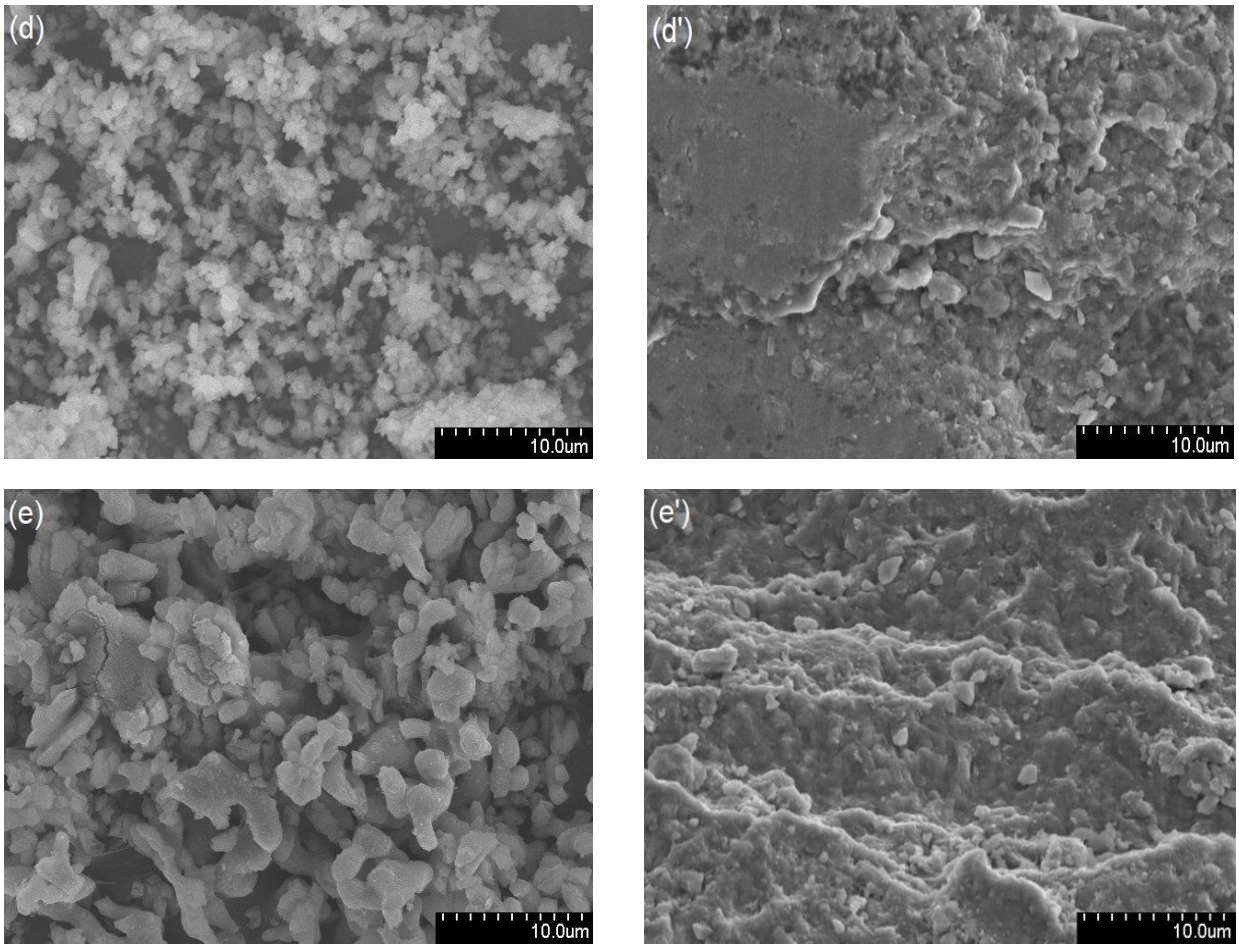

Fig. 7: SEM images of sample; a) uncalcined EW BC; a') uncalcined EW AC; b) 600°C BC; b') 600°C AC; c) 700°C BC; c') 700°C AC; d) 800°C BC; d') 800°C AC; e) 900°C BC; e') 900°C AC.

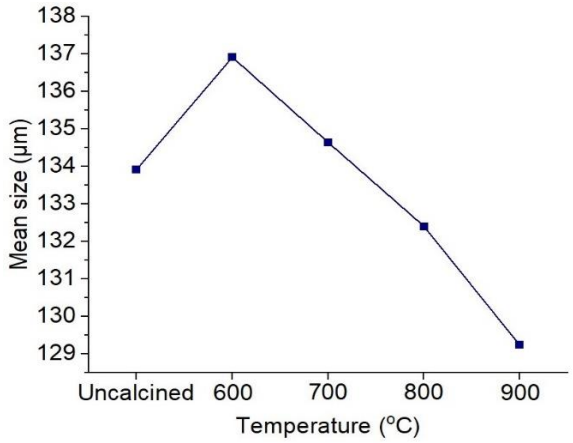

Fig. 8.: Mean size vs calcination temperature graph.

Using Image J, it is possible to see how thermal decomposition affects the mean size of CaO and EW. Uncalcined EW has a mean size slightly below calcined powder at 600°C, which is 133.92±912µm. The mean size of CaO produced from calcinations at 600°C and 700°C is 136.91±19.51µm and 134.64±12.33µm respectively. Eggshells were calcined at 800°C and 900°C respectively, and the results showed that the mean size was 132.41±14.31µm and 129.25±11.68µm. The trend graph in Fig. 8 reveals that uncalcined EW means size with 600°C and 700°C only shows slightly different. It shows that at both temperatures, no significant change in mean size result, while when calcination temperature increase to 800°C and 900°C, the mean size of both powders for both temperatures is lower than uncalcined EW. It shows that high temperatures can reduce the mean size of EW rather than temperatures below 800°C. For the trend in the graph, from 600°C, the line gradually decreased until it started to become mild at 800°C. After that, it begins to decrease until it approaches 900°C gradually. However, the mean size of CaO is not significantly affected by keeping calcinations shorter than 4 hours. The crystalline size of CaO produced from eggshell calcinations at 800°C and 900°C for less than 4 hours of holding time does not differ significantly. Additionally, with increased calcination temperature and holding time, it is evident that the volume of particle sizes decreases[1), 21),29)].

3.3 Hardness

Fig. 9 shows the impact of the indentation load (0.2542 mN) on the hardness of both calcined and uncalcined EW. As the calcination temperature increased, the area of the diamond that was dented also decreased from 34.9 μm^2

for uncalcined EW and 35.9 μm^2 to 30.6 μm^2 for 900°C calcination temperature. The diamond shape shows slightly different sizes for uncalcined, 600°C and 700°C calcination temperatures. However, when the calcination temperature increase to 800°C and 900°C, the size of the diamond shows the most significant difference with uncalcined EW. When the sample is denser and has a higher hardness value, the visible dent in the diamond form has shrunk. It revealed that powder densification happens when pressure causes the holes between powder particles to close and the particles to become denser.

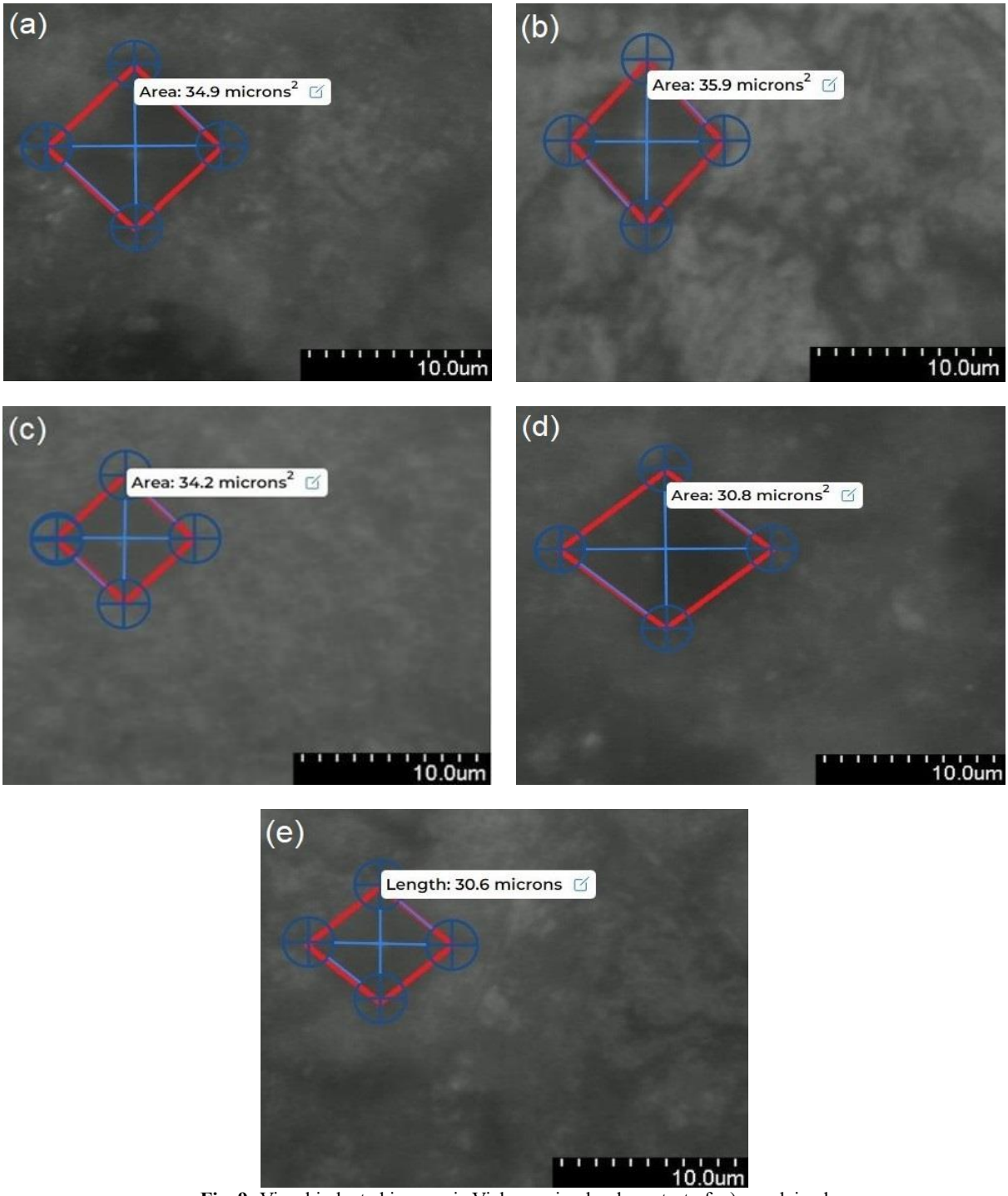

Fig. 9: Visual indented image via Vickers-microhardness test of; a) uncalcined EW; b)600°C; c)700°C; d)800°C; e)900°C.

According to Fig. 10, the hardness value also increases as the calcination temperature rises from 600°C to 900°C. The line began to rise dramatically at 600°C and continued to do so until 700°C, after which it continued to rise slowly until 900°C. The trend of mean hardness values can be traced to creating CaO in significant quantities at

higher calcination temperatures. The steadiest line in the graph represents the amount of CaO that has decomposed. The lowest mean hardness value was recorded at 0.4069 GPa, and the highest at a calcination temperature of 900°C at 0.7607 GPa. The higher the calcination temperature, the narrower the particle size and denser[30),31)] as mentioned in morphological SEM analysis and porosity-density test. Besides, when pressure is applied, the material experiences plastic yielding at particle interactions, which the stress-strain relationship may model. These characteristics help to increase the precision of estimates on how powder densifies in response to pressure and temperature[32)].

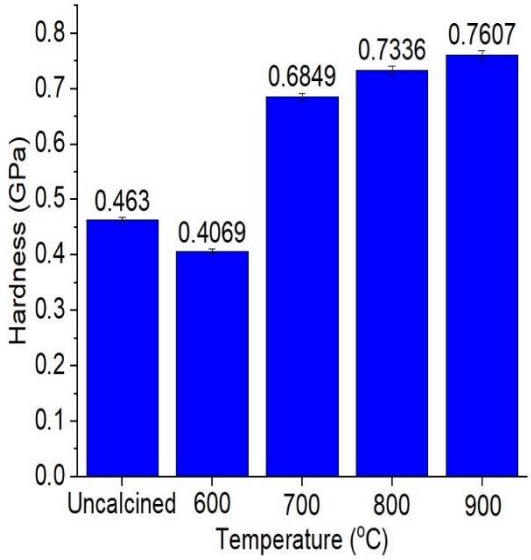

Fig. 10: Hardness vs calcination temperature graph.

Mechanical properties of samples investigated through Vickers microhardness reveal that the denser samples have the highest hardness value of 0.7607 GPa for powder calcined at 900°C. The surface area of the diamond shape dented also decreases as the sample becomes denser and indicates the hardness of the sample. This statement is supported by Fig 9, where the diamond shape size on the sample decreases when the hardness increases. As the hypothesis said, the smaller the diamond shape, the harder the material. Therefore, due to the ease with which EW may be obtained as a catalyst for use in biomedical applications, the investigation of its properties in this experiment was comparable to those of commercial CaO and was thought capable of replacing those of commercial CaO.

4. Conclusion

It was found that varying calcination temperatures impacted the mechanical, microstructural, and physical features of CaO made from eggshell waste. Due to thermal breakdown, the complete conversion of $CaCO_3$ in eggshell waste to CaO was achieved at the highest calcination temperature. As the calcination temperature increased, particle size changed from an irregular concrete-like shape to more rounded edges of interconnected skeleton shape. It is because the particle size of calcined powder also decreases with the smallest mean particle size recorded at 900°C of 129.25±11.68 µm. Besides, the reduction in the mean particle size of CaO powder throughout the calcination temperature also contributes to the increase in density plus a reduction in porosity due to the largest area of surface contact between particles when forced applied during compaction. The highest density was recorded at 2.0974 g/cm^2, with minor porosity of 0.097 vol% for eggshell waste calcined at 900°C. It implies that a higher temperature raises the RD value, leading to a tendency for calcined pellets to become denser.

Acknowledgements

This work was supported by Research Management Centre (RMC) UTHM through Graduate Research Grant (GPPS), vot number H540; and Ministry of Higher Education (MOHE), Malaysia through Fundamental Research Grant Scheme (FRGS), FRGS/1/2019/TK05/UTHM/03/5, vot number K199.

References

1) M.I. Najah, A. Razak, N.A.C.S. Nekmat, S. Adzila, R. Othman, and N. Nordin, "Characterization of calcium carbonate extracted from eggshell waste at various calcination temperature," *IJETER*, **8** (10) 6725–6731 (2020). doi:10.30534/ijeter/2020/16810202.
2) N. Angie, E.M. Tokit, E. M., Abd Rahman, N., Saat, F. A. Z. M., Anuar, F. S., & Mitan, N. M. M. "A preliminary conceptual design approach of food waste composter design," *Evergreen,* **8** (2) 397–407 (2021). doi: 10.5109/4480721.
3) N.M.A. Lestari, "Reduction of CO_2 emission by integrated biomass gasification-solid oxide fuel cell combined with heat recovery and in-situ CO_2 utilization, " *Evergreen,* **6** (3) 254–261 (2019). doi: 10.5109/2349302.
4) T. Zaman, M. Mostari, M.A.A. Mahmood, and M.S. Rahman, "Evolution and characterization of eggshell as a potential candidate of raw material," *Cerâmica*, **64** (370) 236–241 (2018). doi:10.1590/0366-69132018643702349.
5) H. Faridi, and A. Arabhosseini, "Application of eggshell wastes as valuable and utilizable products: A review," *J. Agric. Eng. Res.*, **64** (2) 104–114 (2018). doi: 10.17221/6/2017-RAE.
6) A. Berisha, and L. Osmanaj, "Kosovo scenario for mitigation of greenhouse gas emissions from municipal waste management," *Evergreen*, **8** (3) 509–516 (2021). doi: 10.5109/4491636.
7) B. Priyono, B. Rifky, F. Zahara, and A. Subhan, "Enhancing performance of Li4Ti5O12 with addition

of activated carbon from recycled PET waste as anode battery additives," *Evergreen*, **9** (2) 563–570 (2022). doi:10.5109/4794188.

8) J. Gautron, C. Dombre, F. Nau, C. Feidt, and L. Guillier, "Production factors affecting the quality of chicken table eggs and egg products in Europe. Animal," *Animal*, **16** (1) 1–13 (2022). doi: 10.1016/j.animal.2021.100425.
9) R. Buriak, M. Rudenko, and I. Chornodid, "Marketing research of table eggs market," *Balt. J. Econ. Stud.*, **4** (4), 69–75 (2018). doi: 10.30525/2256-0742/2018-4-4-69-75.
10) S. Mignardi, L. Archilletti, L. Medeghini, and C. De Vito, "Valorization of eggshell biowaste for sustainable environmental remediation," *Sci. Rep.*, **10** (1), 1–10 (2020). doi: 10.1038/s41598-020-59324-5.
11) S.A. Razak, N.A.A.M. Isa, and S. Adzila, "Review on eggshell waste in tissue engineering application," *IJIE*, **14** (4), 64–80 (2022). doi: 10.30880/ijie.2022.14.04.007.
12) S. Sethupathi, Y.C. Kai, L.L. Kong, Y. Munusamy, M.J.K. Bashir, and N. Iberahim, "Preliminary study of sulfur dioxide removal using calcined egg shell," *MJAS,* 21 (3) 719–725 (2017). doi:10.17576/mjas-2017-2103-21.
13) Y.C. Moh, and L. Abd Manaf, "Overview of household solid waste recycling policy status and challenges in Malaysia," *Resour Conserv Recycl*, **82** (6) 20–61 (2014). doi:10.1016/j.resconrec.2013.11.004.
14) A. Shwetha, Dhananjaya, S. M. Shravana Kumara, and Ananda, "Comparative study on calcium content in egg shells of different birds, " *Int. J. Zool.*, **3** (4) 31–33 (2018). doi:archives/2018/vol3/issue4/3-4-18.
15) J. Ruiz, and C.A. Lunam, "Ultrastructural analysis of the eggshell: Contribution of the individual calcified layers and the cuticle to hatchability and egg viability in broiler breeders," *Br. Poult. Sci.*, **41** (5) 584–592 (2000). doi: 10.1080/713654975.
16) I. Abdulrahman, H.I. Tijani, B. Mohammed, H. Saidu, H. Yusuf, M.N. Jibrin, and S. Mohammed, "From garbage to biomaterials: An overview on egg shell based hydroxyapatite, " *J. Mater.*, **2014** (2) 1–7 (2014). doi: 10.1155/2014/802467.
17) S. Hartini, Y. Fiantika, Y., Widharto, and M. Hisjam, "Optimal treatment combination for dishwashing liquid soap based on waste cooking oil according to the requirement of indonesian quality standards," *Evergreen*, **8** (2) 492–498 (2021). doi:. 10.5109/4480734.
18) N.Y. Yahya, J.X. Chan, and N. Ngadi, "Biosorption of chromium (VI) ions using sustainable eggshell impregnated pandanus amaryllifolius roxb. biosorbent," *Evergreen,* **8** (1) 146–155 (2021). doi: 10.5109/4372271.
19) Dwivedi, S. P., Maurya, N. K., & Maurya, M. (2019). "Assessment of hardness on AA2014/eggshell composite produced via electromagnetic stir casting method" *Evergreen,* **6** (4) 285–294 (2019). doi: 10.5109/2547354.
20) A. Razak, N.M. Isa, and S. Adzila, "Synthesis of calcium phosphate extracted from eggshell waste through precipitation method," *Biointerface Res. Appl. Chem.*, **11** (6) 15058–15067 (2021). doi: 10.33263/BRIAC116.1505815067.
21) R. Rohim, R. Ahmad, N. Ibrahim, N. Hamidin and C. Z.A. Abidin, "Characterization of calcium oxide catalyst from eggshell waste," *Adv. Environ. Biol.*, **8** (22) 35–38 (2014). doi: A417895428/AONE?u=anon~17ee0c31&sid=googleScholar&xid=5f16a191.
22) S. Hassanajili, A.K. Pour, A. Oryan and T.T. Khozani, "Preparation and characterization of PLA/PCL/PHA composite scaffolds using indirect 3D printing for bone tissue engineering," *Mater. Sci. Eng. C*, **104** 109960 (2019). doi:10.1016/j.msec.2019.109960.
23) S. Adzila, A. Razak, N. Mat Isa, N.S. Ruslan, and M.A. Selimin, "Review of various hydroxyapatite coating methods on SS316L foam for biomedical application," *JAMEA*, **2** (1), 13–28 (2021). doi: 10.30880/jamea.2021.02.01.002.
24) M.I. Najah, R. Aisyah, S. Adzila, and R.H.A. Haq, "Mechanical properties of calcium phosphate reinforced polyhydroxyalkanoate (PHA) biocomposite," *J. Thermoplast. Compos. Mater.*, **0** (0), 1–18 (2022). doi: 10.1177/0892705722112818.
25) T. Harvey, T. Honeyands, D. O'dea, and G. Evans, "Sinter strength and pore structure development using analogue tests," *ISIJ International*, **60** (1) 73–83 (2020). doi: 10.2355/isijinternational.ISIJINT-2019-247.
26) V. Kyselová, L. Jílková, and K. Ciahotný, Decrease in the adsorption capacity of adsorbents in the high-temperature carbonate loop process for CO_2 capture. *Crystals*, **13** (4) 1–14 (2023). doi: 10.3390/cryst13040559.
27) S. V. R. Tosee, I. Faridmehr, C. Bedon, L. Sadowski, N. Aalimahmoody, M. Nikoo, and T. Nowobilski, "Metaheuristic prediction of the compressive strength of environmentally friendly concrete modified with eggshell powder using the hybrid ANN-SFL optimization algorithm," *Mater.*, **14** (20) 1–20 (2021). doi: 10.3390/ma14206172.
28) W. Zhang, C. Li, Z. Ma, L.Yang, and H. He, "Effects of calcination temperature on properties of 0.5% Al-3% In-TiO_2 photocatalyst prepared using sol-gel method," *J. Adv. Oxid. Technol.*, **19** (1) 119–124 (2016). doi: 10.1515/jaots-2016-0116.
29) M. Kumari, B. Sarkar, and K. Mukherjee, "Nanoscale calcium oxide and its biomedical applications: A comprehensive review," *Biocatal. Agric. Biotechnol.*, **47** (1) 1–14 (2022). doi: 10.1016/j.bcab.2022.102506.
30) R. Aisyah, M. I. Najah, and S. Adzila, "Study of hardness and density of Polyhydroxyalkanoate (PHA) reinforced with Biphasic Calcium Phosphate

(BCP) from eggshell waste, " *The Engineer Story*, **1** (1), 9-11(2023). doi: resources/paper/vol-1/TES-1-9-11.pdf.

31) I. P. T. Indrayana, L. A. Tjuana, and M. T. Tuny, "Nanostructure and optical properties of Fe_3O_4: Effect of calcination temperature and dwelling time," *JPCS*, **1341** (8) 1–10 (2019). doi: 10.1088/1742-6596/1341/8/082044.

32) R. Ahmad, R. Rohim and N. Ibrahim, "Properties of waste eggshell as calcium oxide catalyst, " *Appl. Mech. Mater.*, **754-755** (2015), 171–175 (2015). doi: 10.4028/www.scientific.net/AMM.754-755.171.